Xylem resistance to embolism: presenting a simple diagnostic test for the open vessel artefact

Jose Manuel Torres Ruiz, Hervé Cochard, Brendan Choat, Steven Jansen, Rosa Ana Lopez Rodriguez, Ivana Tomášková, Carmen M. Padilla-Díaz, Eric Badel, Régis Burlett, Andrew King, et al.

Postprint of: New Phytologist (2017) doi: 0.1111/nph.14589

Xylem resistance to embolism: presenting a simple diagnostic test for the open vessel artefact

Torres-Ruiz JM*[1], Cochard H[2], Choat B[3], Jansen S[4], López R[2,3],Tomášková I[5], Padilla-Díaz CM[6], Badel E[2], Burlett R[1], King A[7], Lenoir N[8], Martin-StPaul NK[9] and Delzon S[1].

***Author for correspondence:**
José M. Torres-Ruiz
email: torresruizjm@gmail.com; telephone: +00330540006973.

[1] BIOGECO, INRA, Univ. Bordeaux, 33615 Pessac, France.

[2] PIAF, INRA, Univ. Clermont-Auvergne, 63100 Clermont-Ferrand, France.

[3] Western Sydney University, Hawkesbury Institute for the Environment, Richmond, NSW 2753, Australia

[4] Ulm University, Institute of Systematic Botany and Ecology, Albert-Einstein-Allee 11, 89081 Ulm, Germany

[5] Faculty of Forestry and Wood Sciences, Czech University of Life Sciences, Kamýcká 129, 165 00 Praha 6 – Suchdol, Czech Republic

[6] Instituto de Recursos Naturales y Agrobiología de Sevilla (IRNAS, CSIC), Avenida Reina Mercedes, 10, 41012, Sevilla, Spain

[7] Synchrotron SOLEIL, L'Orme de Merisiers, Saint Aubin-BP48, Gif-sur-Yvette CEDEX, France.

[8] CNRS, University of Bordeaux, UMS 3626 Placamat F-33608 Pessac, France.

[9] INRA, UR629 Ecologie des Forêts Méditerranéennes (URFM), Avignon, France.

Number of words main body: 5257

Tables: 1 // Figures: 6 (3 of them in colour) // Support. Information: 1 figure.

Summary

- Xylem vulnerability to embolism represents an essential trait for evaluating the impact of hydraulics in plant function and ecology. The standard centrifuge technique is widely used for constructing vulnerability curves although its accuracy when applied to long-vesseled species remains under debate.
- We developed a simple diagnostic test to determine if the open-vessel artefact influences centrifuge estimates of embolism resistance. Xylem samples from three species with differing vessel lengths were exposed to less negative xylem pressures via centrifugation than the minimum pressure the sample had previously experienced. Additional calibration was obtained from non-invasive measurement of embolism on intact olive plants by X-Ray microtomography.
- Results showed artefactual decreases in hydraulic conductance (k) for segments with open vessels when exposed to a less negative xylem pressure than the minimum pressure the sample had previously experienced. X-Ray microtomography indicated that most of the embolism formation in olive occurs at xylem pressures below -4.0 MPa, reaching 50% loss of hydraulic conductivity at -5.3 MPa.
- The artefactual reductions in k induced by centrifugation underestimate embolism resistance data of long-vesseled species. A simple test is suggested to avoid this open vessel artefact and to ensure the reliability of this technique in future studies.

Keywords: Artefact, centrifuge technique, embolism, micro-CT, olive, xylem.

Introduction

The continuous water column that connects the soil and the upper portions of the plants through the xylem is exposed to negative pressures induced by the water evaporation at the leaf surface. Water can be pulled up from the soil through the entire plant system thanks to the strong cohesive forces between water-molecules (Dixon, 1914). Under water deficit, the relative water content of the soil decreases, inducing a more negative soil water potential, and the negative pressure inside the water conducting xylem tissue may become interrupted by gas bubbles. These bubbles (emboli) can expand to block conduits and reduce long-distance vascular transport of water. As the number of gas-filled conduits increases, the xylem hydraulic conductance (k, kg s^{-1} MPa^{-1}) decreases until water flow stops, causing desiccation of plant tissues and eventually plant death under severe and prolonged droughts. Failure of the plant hydraulic system is now considered to be the principal mechanism of drought-induced plant mortality (Brodribb & Cochard 2009; Brodribb *et al.,* 2010; Urli *et al.,* 2013; Salmon *et al.* 2015; Anderegg *et al.,* 2016). Given the narrow hydraulic safety margins within which many plants operate (Choat *et al.,* 2012), evaluating the resistance to embolism across plant species is essential to predict future mortality events and shifts in species distribution ranges due to climate change with more intense and severe drought events (IPCC, 2014).

The resistance to xylem embolism is typically assessed by constructing vulnerability curves, which represent the variation in specific hydraulic conductivity (K_s, kg s^{-1} MPa^{-1} m^{-1}) as a function of xylem water potential (Sperry *et al.*, 1988; Cochard *et al*., 2009; Torres-Ruiz *et al.* 2017). During the last few decades, a variety of methods have been developed to determine the loss of K_s in xylem samples exposed to increasing levels of water stress (see Cochard *et al.,* 2013 for a review). Although there is general consensus about centrifuge methods to construct vulnerability curves for species with short conduits (e.g., conifer species), the application of appropriate methods for long-vesseled species remains a subject of debate, especially with regards to the standard centrifuge technique (Alder *et al.,* 1997; Jacobsen & Pratt 2012; McElrone et al. 2012; Tobin *et al*., 2013; Torres-Ruiz *et al.*, 2014; Hacke *et al*., 2015). This technique is based on spinning xylem samples in a custom-built rotor that induces a wide range of pressures at the centre of a sample. In contrast to the Cavitron method (Cochard *et al*., 2005), no water flow is induced through the sample during spinning in the standard centrifuge technique. Each pressure applied may induce a certain loss of

conductivity that is determined gravimetrically with a custom built device (see e.g., Torres-Ruiz *et al.* 2012) or with a commercial instrument relying on Coriolis type mass-flow meters (e.g., Xyl'em embolism meter; Bronkhorst, Montigny-les-Cormeilles, France). The debate is centred on high losses of K_s that the centrifuge technique induces at relatively mild xylem pressures for long-vesseled species, which results in exponential vulnerability curves (the so called 'r-shaped' curves). These curves have been interpreted as a methodological artefact resulting from the presence of open vessels, i.e. vessels that have no vessel end within the stem segment (Choat *et al.,* 2010; Cochard *et al.,* 2010; Torres-Ruiz *et al.,* 2014). However, other authors consider these curves to be a reliable estimate of embolism resistance in these species, i.e. the occurrence of significant embolism within very moderate ranges of water stress (Christman *et al*. 2012; Sperry *et al.,* 2012; Hacke *et al.,* 2015). The discrepancy in these two interpretations impedes our progress in understanding the role of hydraulics in plant function (Delzon & Cochard, 2014) and generates confusion regarding the results and conclusions reached in the field of plant hydraulics. Much efforts have been devoted to clarify whether there is an open-vessel artefact with the standard-centrifuge technique, but contradictory conclusions have been reached even when working with the same plant species. For example, contrasting vulnerability curves and resistances to embolism have been observed for Olive (*Olea europaea*) depending on the technique used for assessing the degree of embolism. While observations with high-resolution computed tomography indicate that embolism does not occur in Olive stems until a certain threshold in xylem pressure is reached (approx. -3.0MPa) and that vulnerability curves of this species show sigmoidal shapes (i.e., a so called 's-shaped' curve; Torres-Ruiz *et al.,* 2014), a recent study reported significant decreases in K_s at relatively high xylem water potentials (Hacke *et al.,* 2015), suggesting r-shaped behaviour and the high embolism vulnerability of this species.

Contrasting conclusions regarding the reliability of the standard centrifuge technique have also been attributed to differences in the centrifuge rotor design used for the measurements (Hacke *et al*. 2015). Briefly, there are two custom rotor designs in use, the original rotor of Alder *et al.* (1997) and the Cavitron rotor (Cochard *et al*., 2005). These designs differ mainly in the way samples are secured and how sample ends are immersed in solution during the spinning. The possible effects of the rotor design on vulnerability curves have been evaluated by Torres-Ruiz *et al.* (2014), who

concluded that both designs produce biased results (overestimated vulnerability to embolism) when samples contain open vessels. Samples in Torres-Ruiz et al. (2014) were cut in two pieces for measuring K_s gravimetrically after spinning, and the appropriateness of this protocol has been questioned by some authors (Hacke *et al.* 2015). Although some intraspecific variation in resistance to embolism could be expected between studies due to the use of different plant material, varieties, seasonality, growth conditions, etc., the large discrepancies observed for species such as olive warrant further investigation.

Typically, resistance to embolism has been assessed by inducing decreasing xylem pressures and determining the corresponding losses in *k*. However, when using a centrifuge method with stem or root segments, it is not possible to determine with certainty that such losses in *k* reflect patterns of embolism that occur *in situ* or if they come from an artefact due to the presence of open-vessels (Fig. 1). By using alternative techniques that allow the direct observation of xylem embolism in a non-invasive manner, such as MRI (Holbrook *et al.,* 2001; Kaufmann *et al.,* 2009; Choat *et al.,* 2010) and X-ray microtomography (micro-CT; Cochard *et al.,* 2015; Torres-Ruiz *et al.,* 2015a, 2016; Bouche *et al.,* 2016; Choat *et al.,* 2016), the open-vessel artefact can be avoided and the process of embolism formation evaluated with greater certainty. As access to some of these non-invasive techniques can be restricted, we propose here a simple alternative test to diagnose the probability of an open vessel artefact occurring and thus ensuring the accuracy of the standard centrifuge technique for a given species. This consists of spinning xylem samples to a less negative pressure than the minimum xylem pressure (i.e. water potential) experienced previously under native conditions or during the progressive dehydration of the plant (Fig. 1). As it is unlikely that embolism will be induced at a less negative pressure, any decrease in K_s before and after the spinning of the sample should represent an experimental artefact.

The aim of this study was to test if K_s values resulting from the standard centrifuge technique are influenced by the presence of open vessels in stem samples with a different vessel anatomy. For this, xylem samples from three vessel-bearing species with contrasting proportions of open vessels were progressively dehydrated to a given xylem pressure. After measuring their K_s gravimetrically, they were exposed to a less negative xylem pressure by using the standard centrifuge technique, and their K_s measured again. Measurements were undertaken with both rotor designs (‘original

design' Alder *et al.,* 1997 and 'Cavitron design' Cochard *et al*., 2005) to evaluate the effects of the rotor type on the results. In addition, embolism resistance in olive trees was determined in intact plants by using micro-CT and compared to earlier centrifuge measurements for this species.

Material and methods

Plant material

Three species with different vessel length distributions were used in this study. Two relatively long-vesseled species: *Olea europaea* Linnaeus and *Quercus palustris* Muenchh, and one relatively short-vesseled species: *Betula pendula* Roth (Ennajeh *et al.,* 2011; Torres-Ruiz *et al.,* 2014). Samples from *Q. palustris* and *B. pendula* were collected from mature individuals located near the campus of University of Bordeaux (France) for measurements with the Cavitron rotor design, and at the Blue Mountains Botanic Garden (NSW, Australia) for measurements with the Alder rotor design. For *O. europaea,* two to three year old saplings were ordered, repotted into 1.5-L pots and grown for two months under well-watered conditions and at ambient light and temperature at the University of Bordeaux (France) and at the Hawkesbury Institute for the Environment (NSW, Australia). A subset of these olive saplings was transported to the SOLEIL synchrotron (Paris, France) in April 2015 for direct micro-CT visualization of embolism formation while the saplings were progressively dehydrated.

Presence of open vessels

The presence of open vessels was determined in similar samples (i.e. similar length, diameter, age and position in the tree) collected from the same branches (for *B. pendula* and *Q. palustris*) or similar saplings (for *O. europaea*) to those used for evaluating the open-vessel artefact in both rotor designs (i.e. 15 or 40 cm long depending on the rotor design). Samples were injected with air at low pressure (50-100 kPa) while its apical end was immersed in water (Greenidge 1952; Zimmerman & Jeje, 1981) to check for the presence of open vessels. In those species for which a continuous flow of air bubbles was detected, the percentage of open vessel was determined by applying the silicone injection method (Hacke *et al.,* 2007). New samples, and not the ones used for evaluating the open-vessel artefact, were used to perform these measurements to avoid the effect of any potential damage to the vascular system caused by the centrifugation

itself could have on the final results. Xylem samples were first flushed basipetally with 10 mM KCl and 1 mM $CaCl_2$ solution at 0.15 MPa for 45 min to remove embolism. Samples were then injected under 30-50 kPa pressure overnight with a 10:1 silicone:hardener mix (RTV-141; Rhodia, Cranbury, NJ, USA). A fluorescent optical brightener (Ciba Uvitex OB; Ciba Specialty Chemicals, Tarrytown, NY, USA) mixed with chloroform 1% (w/w) was added to the silicone (one drop per gram) for the detection of silicone-filled vessels in transverse sections under fluorescent microscopy (NanoZoomer; Hamamatsu Photonics, Japan). After 2–3 days allowing the silicone to harden, the two sample ends were sectioned with a sliding microtome at 5 mm from each end. As the silicone mixture does not penetrate pit membranes but fills entirely the vessel lumina starting from the injection site, the amount of open vessels through the sample was determined by counting the fraction of silicone-filled vessels at both sample ends.

Evaluation of the open-vessel artefact

Since embolism can theoretically not be induced via air-seeding by exposing the xylem to less negative water potentials than the minimum water potential previously experienced, the open-vessel artefact was evaluated by spinning xylem samples at a velocity that corresponded to a less negative pressure than the pressure reached by stem branches during a previous drought treatment. Two different rotor designs, the original rotor design (Alder *et al.* 1997) and the Cavitron (Cochard *et al*. 2005), were used to check if the type of rotor could have an effect on the results. Several branches (≥ 2.0 m in length) of *B. pendula* and *Q. palustris* were collected in the early morning and transported to the lab where they were allowed to dehydrate progressively (up to 5 hours, depending on the species). For *O. europaea* (var. *arbequina* for the Cavitron design and *manzanilla* for the original one), saplings were exposed to increasing water stress by withholding irrigation. The xylem pressure of each branch and sapling was monitored regularly by measuring the leaf water potential with a Scholander-type pressure chamber (DGMeca, Gradignan, France) on two leaves per branch or sapling that were previously bagged up (at least 1h before taking the water potential measurements). Once the xylem pressure reached values of -1.8 MPa or lower, a xylem sample was immediately collected for K_s measurements. Samples were collected according to the experimental protocol of Torres-Ruiz *et al.* (2015a) to avoid the excision artefact described by Wheeler *et al.* (2013). Briefly, the entire branch or

sapling was progressively recut under water so that the xylem samples were excised once the xylem pressure was released. Depending on the species and the diameter of the rotors used, different sample lengths were used to avoid/ensure the presence of open vessels in the samples, which allowed us to check their effect on K_s after spinning. Thus, for the long-vesseled species (*O. europaea* and *Q. palustris*) excised samples were 15 cm long for both rotor designs, whereas for the short-vesseled one, *B. pendula*, samples were 40 cm long for the Cavitron design and 15 cm long for the original design (40-cm-diameter original rotor not available). K_s for each sample was determined by attaching the samples to a tubing apparatus (Sperry *et al*. 1988; Torres-Ruiz *et al.* 2012) filled with a degassed and ultrapure 10 mM KCl and 1 mM $CaCl_2$ solution. All samples were about 3 to 9 mm in xylem diameter (i.e. without bark) and they included growth rings from previous years. However, no air-seeding fatigue is expected since embolised conduits were not flushed. Before taking measurements, both sample ends were debarked and slightly trimmed under water with a sharp razor blade to adjust the desired length and to clear any accidentally blocked vessels. To account for possible passive uptake of water by the sample, K_s was calculated as the slope of the flow, which was calculated from the linear regression of the pressure gradient for three different pressure heads (between 2.0 and 3.5 kPa) as described by Torres-Ruiz *et al.* (2012). Previous tests showed that the pressure gradients used for our measurements were low enough to avoid displacing air from embolised vessels open at both ends of the segment. Samples were installed in a custom-built rotor of the Alder *et al.* (1997) design (15 cm diameter) or the Cochard *et al.,* (2005) Cavitron design (40 cm). They were then spun for 5 min, with their ends immersed in the same solution as used for K_s measurements, at a velocity equivalent to a xylem pressure of -1.5 MPa and without inducing any flow through the samples during spinning. To avoid desiccation and to keep the solution in contact with the sample ends when the rotor was stopped, foam pads soaked in the solution used for measurements were placed in the reservoirs of both rotor designs (Tobin *et al.,* 2013). After spinning, samples were removed from the rotor and K_s was measured again. Samples were spun only once ('single-spin centrifuge method', Hacke *et al.,* 2015) to avoid any effect associated with repeated spinning on the same sample. Sapwood area-specific conductivity (K_s) instead of percentage loss of hydraulic conductivity (PLC) values was reported to avoid any possible drift by errors when calculating maximum K_s (Sperry *et al.,* 2012). The native K_s of five extra olive saplings

was also measured in order to test for possible changes in K_s at relative high water potential.

Checking for possible embolism repair during xylem relaxation

The relaxation of xylem pressure carried out to avoid the excision artefact could favour embolism repair in some species (Trifilò *et al.* 2014). If this was the case for our species, K_s measured for the dehydration treatment would be higher than K_s measured after centrifugation only because partial refilling had occurred with xylem relaxation treatment. In this case lower K_s after spinning could be erroneously interpreted as an artefact. In order to eliminate this possibility we performed an additional phloem girdling treatment, which has been reported to be an effective method to inhibit xylem refilling (Trifilò *et al*. 2014). K_s from girdled and non-girdled samples was measured after xylem relaxation following the same protocol described for the evaluation of the open-vessel artefact. Thus, once the plant material reached a xylem pressure of -1.8 MPa or lower, a group of 5 to 6 samples per species were girdled for their entire length by removing 5-10 mm wide bark rings at 10-15 cm intervals, while a second group of 5 to 8 samples were left intact (control). To prevent desiccation, the exposed wood was immediately covered with a thin layer of silicone grease. For collecting the girdled and control samples, the entire branches were progressively recut under water and the samples excised once the xylem pressure was released. Samples were then attached to the tubing apparatus and K_s measured gravimetrically as described above to check for possible repairing processes (i.e. higher K_s values) occurring in the non-girdled samples.

To determine if the process of connecting and disconnecting or perfusing the samples with the measurement solution could account for a possible decline in conductance after centrifugation, K_s was measured for one of the long-vesseled species (*Olea europaea*) before (K_{s1}) and after (K_{s2}) disconnecting the samples. For this purpose, samples were kept in water for a similar time as the duration of the centrifuge spinning (i.e., 5 min) and then reconnected to the tubing of the conductivity apparatus.

Resistance to embolism in intact olive saplings: X-ray microtomography.

Synchrotron based computed X-ray microtomography (micro-CT) was used to visualize embolised and water filled conduits in the current-year shoots of intact olive saplings (*Olea europaea*, var. *arbequina*). A total of 15 olive saplings were scanned between 8 and 12 April 2015 at the French synchrotron facility SOLEIL (Paris, France) using the

micro-CT beamline (PSICHE). Two weeks prior to the scans, irrigation was withheld progressively in different saplings in order to generate a wide range of xylem water potentials at the time of the scanning.

Once at the synchrotron and 1.5 hours before each scan, two leaves, located 20 mm below the scanned area, were wrapped in a plastic bag and covered with aluminium foil to prevent transpiration and allow the equilibrium between leaf and stem water potential. Water potential was then measured on these bagged leaves right before the scan with a Scholander-type pressure chamber (Precis 2000, Gradignan, France). Current-year shoots were scanned using a high flux (3.1011 photons mm^{-2}) 25 keV monochromatic X-ray beam. The projections were recorded with a Hamamatsu Orca Flash sCMOS camera equipped with a 250 μm thick LuAG scintillator and visible light optics providing an effective pixel size of 3 microns. The complete tomographic scan included 1,500 projections, 50 ms each, for a 180° rotation. Samples were exposed for 75 s to the X-ray beam. Tomographic reconstructions were performed using PyHST2 software (Mirone *et al.*, 2014) using the Paganin method (Paganin, 2006).

The loss of theoretical conductance k was determined from a transverse 2D micro-CT slice taken from the centre of the scan volume by estimating the theoretical k of each sapling stem based on the conduit dimensions of embolised and functional conduits. A final scan was carried out on each shoot after cutting it in air at approximatively 5 mm above the scan area. Because the xylem was still under negative pressure, we therefore induced embolism in all remaining functional vessels in order to create a reference scan ('cutting artefact', Wheeler *et al.,* 2013; Cochard *et al.,* 2015; Torres-Ruiz *et al.,* 2015a; Choat *et al*., 2016), while distinguishing at the same time a small amount of living vessels (i.e., not fully developed), which were excluded from our calculations. The maximum theoretical k (k_{max}, kg s^{-1} MPa^{-1}) of each sapling was then calculated according to the Hagen-Poiseuille equation:

$$k_{max} = \Sigma \pi D^4 / 128 \eta \quad (1)$$

where D is the conduit diameter and η is the viscosity of water. The k for each sapling and xylem pressure was calculated by subtracting the total k of all the embolised vessels from its k_{max}, being the percent loss of k (PLC) calculated as:

$$PLC = 100 \times (1 - k / k_{max})$$

To account for a small amount of embolised vessels that are typically observed at high xylem water potentials, the vulnerability curve was fitted with a modified Weibull function (Neufeld *et al.,* 1992) to include an additional independent parameter (Torres-Ruiz *et al.,* 2015b):

$$PLC = (100 - y_0)(1 - e^{-(\frac{x}{b})^c}) + y_0$$

with being x the xylem pressure, b the xylem pressure for a PLC of 63%, c a dimensionless parameter controlling the shape of the curve and y_0 the PLC at a xylem water potential of 0 MPa. The air entry pressure (P_e), indicating the threshold xylem pressure at which loss of conductivity begins to increase rapidly (Meinzer *et al.,* 2009), was computed from the x-intercept of the tangent through the midpoint of the vulnerability curve.

Statistics

Differences within a species in mean K_s values measured both in girdled and non-girdled (control) samples, and before and after spinning were tested with paired t-tests after testing for normality and homogeneity of variances. The tests were made at a probability level of 5%. All analyses were performed using Sigmaplot (SPSS Inc., Chicago, IL, USA).

Results

The air-injection method confirmed the presence of open vessels in 15-cm long samples for the two long-vesseled species (*Q. palustris* and *O. europaea*), whereas no open vessels were detected for *B. pendula* in the 15 cm and 40 cm-long stem segments. Results from the silicone injection technique showed that the percentage of open vessels for the 15 cm-long samples of *Q. palustris* and *O. europaea* (Fig. 2) was 70.7±7.3% (n = 4) and 27.0±8.4% (n = 4), respectively.

The progressive dehydration induced mean xylem pressures between -1.8 and -2.5 MPa before taking K_s measurements (Table 1) for the three species studied. A significant decrease in K_s was observed for the two long-vesseled species when samples were exposed in a centrifuge to a less negative xylem pressure than the minimum pressure previously experienced by the entire plant or large branches (i.e. -1.5 MPa, Fig.

3), independent of the rotor design. Thus, *O. europaea* showed a mean decrease in K_s of 46.8±8.1% and 54.3±4.9% using the Cavitron and the original rotor, respectively, whereas for *Q. palustris* this decrease reached 66.6±9.1% and 61.4±6.7%, respectively. In contrast, samples of the short-vesseled species *B. pendula* showed similar conductances before and after spinning for both rotor types.

There was no evidence that the relaxation of the xylem pressure carried out to avoid the excision artefact resulted in embolism repair; similar K_s values were observed in girdled and control xylem-relaxed samples for the three species evaluated (Fig. 4a). Differences in K_s values reported in Fig. 2 and 4 are due to the fact that both sets of measurements were carried out at a different time. No differences in K_s were found between control samples that were kept in water for 5 minutes and then reconnected to the conductivity apparatus (Fig. 4b).

Micro-CT images from drought stressed olive saplings showed that the PLC remained relatively low (12.6%) when xylem pressure decreased from -0.4 to -4.0 MPa (Fig. 5). However, images showed a significant loss of hydraulic conductance (PLC = 75.7%) when xylem pressure reached -6.2 MPa. Thus, the vulnerability curve for olive obtained by direct micro-CT observation showed only a slight increase in PLC up to -4.0 MPa (Fig. 6). As the P_e values indicated, at xylem pressures below -4.0 MPa the loss of k started to increase steeply, reaching 50% loss of k (P_{50}) at -5.3 MPa.

Discussion

All xylem samples with some proportion of their vessels open at both cut ends showed a decrease in K_s when they were exposed to a less negative xylem pressure than the minimum pressure previously experienced during the progressive dehydration of the branch samples (*Q. palustris*) or the intact plant (*O. europaea)*. This observation was found by applying the standard centrifuge for both the Alder and Cavitron rotor designs. Thus, *Q. palustris* and *O. europaea* showed a mean decrease in K_s of 70.8 and 49.6%, respectively, when using the Alder rotor design, and 61.4 and 54.3%, respectively, when using the Cavitron design. As embolism should not be induced by exposing the xylem to less negative pressures, the observed reductions in K_s are likely due to experimental artefact. Indeed, the control test showed that such reductions were not caused by wounding responses, perforation plate morphology, clogging or embolism induction while samples were loaded and unloaded in the tubing conductivity apparatus,

or by other artefacts during handling and sample preparation. Also, direct micro-CT observations show little embolism formation in intact plants at a xylem pressure of -1.5 MPa providing further evidence that this artefact was the main cause of reductions in K_s after centrifugation. Samples of *B. pendula* that did not contain any open vessels exhibited no change in K_s before and after being spun in both rotors. These results are consistent with the hypothesis that the experimental artefact causing significant embolism at xylem pressures near zero is associated with the presence of open xylem vessels in the test segment. This artefact was previously reported when applying the standard centrifuge technique to long-vesseled species (Choat *et al.,* 2010; McElrone *et al.,* 2012; Choat *et al.,* 2016), with evidence showing that the shape of the vulnerability curves obtained with this method varied with the amount of open vessels (Torres-Ruiz *et al.*, 2014). A possible explication of the observed decreases in K_s after spinning could be the ease with which water can drain from open vessels during spinning due to asymmetric vessel morphology. In particular, it is well known that the inner diameter of vessel lumina shows considerable variation along its axis (Akachuku, 1987; Balaz *et al*,. 2016). Moreover, xylem vessels are not the ideal 'pipes' running perfectly straight but show some tortuosity (Braun 1959; Tyree and Zimmermann 2002). Therefore, it is likely that during the spinning minor pressure differences occur between both ends, with air entering one end, and water draining out of the other one.

The present study provides additional evidence that the standard centrifuge technique is prone to underestimating resistance to embolism in samples with open vessels, regardless of rotor design. This is consistent with a survey of more than 1,200 vulnerability curves (Cochard *et al.*, 2013), illustrating that exponential-shaped curves are remarkably frequent for species with long xylem vessels when they were obtained with a centrifuge methods, i.e. both the standard-centrifuge and the Cavitron method.

Our findings contrast with the conclusion that the standard centrifuge technique accurately measures vulnerability curves of long-vesseled species such as grapevine and olive (Jacobsen and Pratt, 2012; Hacke *et al.*, 2015; Pratt *et al.*, 2015). This conclusion was based on the agreement between native K_s and PLC values from dehydration-based measurements and from single-spin centrifugations (Fig. 6 in Hacke *et al.,* 2015). However, no native K_s values or direct observations were reported in Hacke *et al.* (2015) for xylem pressures between 0.0 and -1.0 MPa, i.e. the pressures at which the

largest changes in K_s are expected according to their exponential-shaped curve. Also, their measurements were conducted in September and October, i.e. late summer. Since the trees sampled by Hacke et al. (2015) could have been exposed to lower water potentials during mid-summer, they could have experienced some embolism that would not correspond with the water potential measured at the time of the K_s measurements. These underestimated K_s values at relatively high water potentials could therefore agree with the reduced centrifuge K_s values resulting from an open-vessel artefact and, therefore, be erroneously considered as an evidence for rejecting the occurrence of an open-vessel artefact. Moreover, no effect of the amount of open vessels on the shape of the curve was reported when using 13.5 and 27cm-long samples with different amounts of open vessels (Fig. 4 in Hacke *et al.,* 2015). If the amount of open vessels is relatively high (i.e. >50%) for both stem sizes, vulnerability curves based on samples can be equally biased (Fig. 3 in Hacke *et al.*, 2015). Moreover, a control experiment with samples showing 0% of open vessels is required to confirm that the amount of open vessels has no effect on a vulnerability curve that is based on centrifuge techniques. Similarly low resistances to embolism were observed for 1-yr-old grapevine stems with different percentages of open vessels (Jacobsen & Pratt, 2012). Although some differences in P_{50} could be expected between varieties of grapevine, independent studies carried out on intact grapevine plants by micro-CT have reported considerably higher stem resistances to embolism for *Vitis vinifera* (McElrone *et al.* 2012; Charrier *et al.* 2016).

It is important to highlight that special attention was paid to address previous criticisms from similar tests on the open-vessel artefact, following the latest recommendations and accounting for various sources of error in hydraulic measurements: the use of foam pads to avoid the draining of open vessels (Tobin *et al.,* 2013); single centrifugation of samples ('single-spin' protocol, Hacke *et al.,* 2015); accounting for passive water uptake by samples (Torres-Ruiz *et al.,* 2012); releasing the xylem pressure before excising samples (Wheeler *et al.,* 2013; Torres-Ruiz *et al.,* 2015a); and hydraulic quantification based on K_s values instead of PLC (Sperry *et al.,* 2012). Also, no evidence for embolism repair was detected in any of the three species evaluated, showing similar K_s values between girdled (i.e., samples with their possible refilling mechanism inhibited, see Trifilò *et al*. 2014) and non-girdled (control) samples after relaxing their xylem pressure. Indeed, there is growing evidence from various

449 research groups that the water transport system of plants is generally resistant to air
450 entry for the normal, daily range of pressures the xylem experiences (McElrone *et al.*,
451 2012; Martin-StPaul *et al.,* 2014; Bouche *et al*., 2016; Brodribb *et al*., 2016; Choat *et*
452 *al.*, 2016; Lens *et al*., 2016). A challenge ahead, however, which is at least as important
453 as technical progress in quantifying xylem embolism resistance, includes a better
454 understanding of the actual mechanisms behind drought- and frost-induced embolism
455 formation in plant xylem, in particular air-seeding (Charrier *et al.*, 2014; Jansen and
456 Schenk, 2015; Schenk et al., 2016).

457 Our results do not undermine the standard centrifuge technique, but highlight the
458 importance of conducting simple checks on plant material in order to ensure that
459 embolism resistance is measured accurately. These checks are not necessary for tracheid
460 bearing species but are advisable for angiosperm species, particularly those known to
461 have long xylem vessels. Only when K_s remains similar before and after spinning at a
462 less negative pressure than the minimum pressure previously experienced by the
463 material can vulnerability curves based on the centrifuge technique be considered as
464 accurate. In fact, the test proposed here would probably have avoided the discrepancy
465 about the shape of the response of k to xylem pressure for olive (Torres-Ruiz *et al*.,
466 2014; Hacke *et al*., 2015). The direct observation of embolism formation in intact olives
467 trees carried out in this study, however, confirms that embolism formation occurs when
468 xylem water potential falls below a threshold value that is reached under severe drought
469 conditions, supporting its designation as a drought-tolerant species (LoGullo & Salleo,
470 1988; Fernández & Moreno, 1999; Connor & Fereres, 2005; Diaz-Espejo *et al.,* 2012)
471 and the sigmoidal shape of the vulnerability curves of this species (Torres-Ruiz *et al.*,
472 2014), which is consistent with the high-embolism-resistance paradigm proposed by
473 Delzon & Cochard (2014).

474 The use of different varieties, growing conditions, plant sizes, sampling period,
475 etc. is likely to explain some degree of intraspecific variability in P_{50} between studies
476 (this study; Ennajeh *et al.,* 2008; Torres-Ruiz *et al.,* 2013), but not the observation of
477 dramatically contrasting embolism resistance strategies (Torres-Ruiz *et al*., 2014).
478 Indeed, the low variability in P_{50} typically observed within a single species (Martinez-
479 Vilalta *et al.,* 2004; Lamy *et al.,* 2014) and the fact that 'exponential' curves are
480 typically associated with centrifuge methods and long-vesseled angiosperms species

(Cochard *et al.,* 2013) casts further doubt over measurements indicating a low resistance to embolism for olive.

Conclusions

This study demonstrates that the standard centrifuge technique does not accurately measure resistance to embolism in xylem samples with some proportion of open vessels, regardless of the rotor design used. Wood samples with open-vessels showed a significant decrease in K_s after spinning at a less negative xylem pressure than the minimum pressure previously experienced by the plant material, which was not due to embolism formation. Micro-CT observations of intact olive plants confirmed the high-embolism-resistance strategy for Olive, with almost no embolism formation until water potential reaches a certain threshold value. Overall, the findings from this study are in line with earlier evidence that embolism resistance in plants, especially for long-vesseled species, is not as low as previously suggested.

Acknowledgments

We thank the Experimental Unit of Pierroton, UE 0570, INRA, 69 route d'Arcachon, 33612 CESTAS (France), and the Blue Mountains Botanic Garden staff and Robert Spooner-Hart for providing material and technical support. For fluorescent microscopy, we thank the Bordeaux Imaging Center (CNRS-INSERM) and Bordeaux University. Sébastien Marais is acknowledged for technical support with fluorescent microscopy. CMP-D was supported by a scholarship from the Spanish Ministry of Economy and Competitiveness (EEBB-I-15-09191). We thank the PSICHE beamline (SOLEIL synchrotron facility, project 20141229). This work was supported by the programme 'Investments for the Future' ANR-10-EQPX-16, XYLOFOREST) from the French National Agency for Research. BC was supported by an Australian Research Council (Future Fellowship grant no. FT130101115). RL was supported by a Marie Curie fellowship (no. 624473) of the EU FP7 Programme.

Author contributions

JMT-R designed the experiment, carried out the measurements, performed the data analysis and wrote the first manuscript draft. JMT-R, IT, RL, SD, EB and CMP-D collected the plant material and carried out some of the measurements. JMT-R, HC, SD,

BC, SJ, EB, RB, AK, NL and NKS-P assisted with setting up the Synchrotron scans. JMT-R, SJ, BC, HC and SD contributed ideas and assisted substantially with manuscript development.

References

Akachuku AE. 1987. A study of lumen diameter variation along the longitudinal axis of wood vessels in *Quercus ruhra* using cinematography. IAWA Bull (NS) **8**: 41-45.

Alder NN, Pockman WT, Sperry JS, Nuismer S. 1997. Use of centrifugal force in the study of xylem cavitation. *Journal of experimental botany* **48**: 665–674.

Anderegg WRL, Klein T, Bartlett M, Sack L, Pellegrini AFA, Choat B, Jansen S. 2016. Meta-analysis reveals that hydraulic traits explain cross-species patterns of drought-induced tree mortality across the globe. *Proceedings of the National Academy of Sciences,* in press. doi:10.1073/pnas.1525678113.

Balaz M, Jupa R, Jansen S, Cobb A, Gloser V. 2016. Partitioning of vessel resistivity in three liana species. *Tree Physiology* **36**: 1498-1507.

Bouche PS, Delzon S, Choat B, Badel E, Brodribb T, Burlett R, Cochard H, Charra-Vaskou K, Lavigne B, Li S *et al.* 2016. Are needles of *Pinus pinaster* more vulnerable to xylem embolism than branches? New insights from X-ray computed tomography. *Plant, Cell & Environment* **39**: 860-870. doi: 10.1111/pce.12680

Braun HJ. 1959. Die Vernetzung der Gefässe bei Populus. Zeitschrift für Botanik **47**: 421-434

Brodribb TJ, Bienaimé D, Marmottant P. 2016 Revealing catastrophic failure of leaf networks under stress. *PNAS* **113** (17): 4865-4869.

Brodribb TJ, Bowman D, Nichols S, Delzon S, Burlett R. 2010. Xylem function and growth rate interact to determine recovery rates after exposure to extreme water deficit. *New Phytologist* **188**: 533–542.

Brodribb TJ, Cochard H. 2009. Hydraulic failure defines the recovery and point of death in water-stressed conifers. *Plant Physiology* **149**: 575–584.

542 **Charrier G, Torres-Ruiz JM, Badel E, Burlett R, Choat B, Cochard H, Delmas**
543 **CEL, Domec JC, Jansen S, King A, Lenoir N, Martin-StPaul N, Gambetta**
544 **GA, Delzon S. 2016**. Evidence for hydraulic vulnerability segmentation and lack
545 of xylem refilling under tension. *Plant Physiology* 172: 1657-1668.

546 **Choat B, Badel E, Burlett R, Delzon S, Cochard H, Jansen S. 2016.** Non-invasive
547 measurement of vulnerability to drought induced embolism by X-ray
548 microtomography. *Plant Physiology* **170**:273–282.

549 **Choat B, Drayton WM, Brodersen C, Matthews MA, Schackel KA, Wada H,**
550 **McElrone AJ. 2010.** Measurement of vulnerability to water stress-induced
551 cavitation in grapevine: a comparison of four techniques applied to a long-
552 vesseled species. *Plant, Cell & Environment* **33**: 1502–1512.

553 **Choat B, Jansen S, Brodribb TJ, Cochard H, Delzon S, Bhaskar R *et al.* 2012.**
554 Global convergence in the vulnerability of forests to drought. *Nature* **491**: 752–
555 755.

556 **Christman MA, Sperry JS, Smith DD. 2012.** Rare pits, large vessels, and extreme
557 vulnerability to cavitation in a ring-porous tree species. *New Phytologist*
558 **193**:713-720.

559 **Cochard H, Badel E, Herbette S, Delzon S, Choat B, Jansen S. 2013.** Methods for
560 measuring plant vulnerability to cavitation: a critical review. *Journal of*
561 *Experimental Botany* **64**: 4779–4791.

562 **Cochard H, Damour G, Bodet C, Tharwat I, Poirier M, Ameglio T. 2005.**
563 Evaluation of a new centrifuge technique for rapid generation of xylem
564 vulnerability curves. *Physiologia Plantarum* **124**: 410–418.

565 **Cochard H, Delzon S, Badel E. 2015.** X-ray microtomography (micro-CT): a reference
566 technology for high-resolution quantification of xylem embolism in trees. *Plant,*
567 *Cell & Environment* **38**: 201–206.

568 **Cochard H, Herbette S, Barigah T, Vilagrosa A. 2010.** Does sample length influence
569 the shape of vulnerability to cavitation curves? A test with the Cavitron spinning
570 technique. *Plant, Cell & Environment* **33**: 1543–1552.

Cochard H, Hölttä T, Herbette S, Delzon S, Mencuccini M. 2009. New insights into the mechanisms of water-stress-induced cavitation in conifers. *Plant Physiolgy* **151**:949–54.

Connor, DJ, Fereres E. 2005. The physiology of adaptation and yield expression in olive. *Horticultural Reviews* **34**: 155–229.

Delzon S, Cochard H. 2014. Recent advances in tree hydraulics highlight the ecological significance of the hydraulic safety margin. *New Phytologist* **203**: 355–358.

Diaz-Espejo A, Buckley TN, Sperry JS, Cuevas MV, de Cires A, Elsayed-Farag S, Martin-Palomo MJ, Muriel JL, Perez-Martin A, Rodriguez-Dominguez C *et al*. 2012. Steps toward an improvement in process-based models of water use by fruit trees: a case study in olive. *Agricultural Water Management* **114**: 37–49.

Dixon H. 1914. Transpiration and the Ascent of Sap in Plants. MacMillan, New York.

Ennajeh M, Simoes F, Khemira H, Cochard H. 2011. How reliable is the double-ended pressure sleeve technique for assessing xylem vulnerability to cavitation in woody angiosperms? *Physiologia Plantarum* **142**: 205–210

Ennajeh M, Tounekti T, Ahmedou MV, Khemira H, Cochard H. 2008. Water relations and drought-induced embolism in two olive (*Olea europaea* L.) varieties 'Meski' and 'Chemlali' under severe drought conditions. *Tree Physiolgy* **28**: 971–976.

Fernández JE, Moreno F, 1999. Water use by the olive tree. *Journal of Crop Production* **2**: 101–162.

Greenidge KNH. 1952. An approach to the study of vessel length in hardwood species. *American Journal of Botany*, **39** (8): 570-574.

Hacke UG, Sperry JS, Feild TS, Sano Y, Sikkema EH, Pittermann J. 2007. Water transport in vesseless angiosperms: conducting efficiency and cavitation safety. *International Journal of Plant Sciences* **168**: 1113–1126.

Hacke UG, Venturas MD, MacKinnon ED, Jacobsen AL, Sperry JS, Pratt RB. 2015. The standard centrifuge method accurately measures vulnerability curves of long-vesselled olive stems. *New Phytologist* **205**: 116–127. doi: 10.1111/nph.13017.

602 **Holbrook NM, Ahrens ET Burns MJ, Zwieniecki MA. 2001.** In Vivo Observation of
603 Cavitation and Embolism Repair Using Magnetic Resonance Imaging. *Plant*
604 *Physiology* **126**: 27–31

605 **IPCC. 2014**. Core Writing Team, Pachauri RK, Meyer LA, eds. *Climate Change 2014:*
606 *Synthesis Report. Contribution of Working Groups I, II and III to the Fifth*
607 *Assessment Report of the Intergovernmental Panel on Climate Change, IPCC.*
608 Geneva, Switzerland, 151 pp.

609 **Jacobsen AL, Pratt RB. 2012**. No evidence for an open vessel effect in centrifuge-
610 based vulnerability curves of a long-vesselled liana (*Vitis vinifera*). *New*
611 *Phytologist* **194**: 982-990.

612 **Kaufmann I, Schulze-Till T, Schneider HU, Zimmermann U, Jakob P, Wegner**
613 **LH. 2009.** Functional repair of embolized vessels in maize roots after temporal
614 drought stress, as demonstrated by magnetic resonance *New Phytologist*
615 **184**:245–56. doi: 10.1111/j.1469-8137.2009.02919.x.

616 **Lamy J-B, Delzon S, Bouche PS, Alia R, Vendramin GG, Cochard H, Plomion C.**
617 **2014.** Limited genetic variability and phenotypic plasticity detected for
618 cavitation resistance in a Mediterranean pine. *New Phytologist* **201**:874–886.
619 doi: 10.1111/nph.12556

620 **Lens F, Picon-Cochard C, Delmas C, Signarbieux C, Buttler A, Jansen S, Chauvin**
621 **T, Chacon Doria L, Arco M del, Cochard H, Delzon S. 2016**. Herbaceous
622 angiosperms are not more vulnerable to drought-induced embolism than
623 angiosperm trees. *Plant Physiology* **172**: 661-667

624 **Lo Gullo MA, Salleo S. 1988.** Different strategies of drought resistance in three
625 Mediterranean sclerophyllous trees growing in the same environmental condi-
626 tions. *New Phytologist* **108**: 267–276.

627 **Martínez-Vilalta J, Sala A, Piñol J. 2004.** The hydraulic architecture of Pinaceae – a
628 review. *Plant Ecology* **171**: 3–13.

629 **Martin-StPaul NK, Longepierre D, Huc R, Delzon S, Burlett R, Joffre R, *et al.***
630 **2014.** How reliable are methods to assess xylem vulnerability to cavitation? The
631 issue of "open vessel" artifact in oaks. Tree Physiology, **34**: 894–905

McElrone AJ, Brodersen C, Alsina M, Drayton W, Matthews M, Shackel K, Wada H, Zufferey V, Choat B. 2012. Centrifuge technique consistently overestimates vulnerability to water stress-induced cavitation in grapevines as confirmed with high-resolution computed tomography. *New Phytologist* **196**: 661–665.

Meinzer FC, Johnson DM, Lachenbruch B, McCulloh KA, Woodruff DR. 2009. Xylem hydraulic safety margins in woody plants: coordination of stomatal control of xylem tension with hydraulic capacitance. *Functional Ecology* **23**: 922–930.

Mirone A, Brun E, Gouillart E, Tafforeau P, Kieffer J. 2014. The PyHST2 hybrid distributed code for high speed tomographic reconstruction with iterative reconstruction and a priori knowledge capabilities, Nuclear Instruments and Methods in Physics Research Section B: Beam Interactions with Materials and Atoms **324**: 41–48.

Neufeld HS, Grantz DA, Meinzer FC, Goldstein G, Crisosto GM, Crisosto C. 1992. Genotypic variability of leaf xylem cavitation in water-stressed and well-irrigated sugarcane. *Plant Physiology* **100**: 1020–1028.

Paganin, DM. 2006. Coherent X-Ray Optics, Vol. 6 of Oxford series on synchrotron radiation, Oxford University Press, Oxford.

Pratt RB, MacKinnon ED, Venturas MD, Crous CJ, Jacobsen AL. 2015. Root resistance to cavitation is accurately measured using a centrifuge technique. *Tree Physiology* **35**: 185-196.

Salmon Y, Torres-Ruiz JM, Poyatos R, Martinez-Vilalta J, Meir P, Cochard H, Mencuccini M. 2015. Balancing the risks of hydraulic failure and carbon starvation: a twig scale analysis in declining Scots pine. *Plant, Cell & Environment* **38**: 2575–2588.

Sperry JS, Christman MA, Torres-Ruiz JM, Taneda H, Smith DD. 2012 Vulnerability curves by centrifugation: is there an open vessel artefact, and are "r" shaped curves necessarily invalid? *Plant, Cell & Environment* **35**: 601–610.

Sperry JS, Donnelly JR, Tyree MT. 1988. A method for measuring hydraulic conductivity and embolism in xylem. *Plant, Cell & Environment* **11**: 35–40.

662 **Tobin MF, Pratt RB, Jacobsen AL, De Guzman M. 2013.** Xylem vulnerability to
663 cavitation can be accurately characterized in species with long vessels using a
664 centrifuge method. *Plant Biology* **15**: 496–504.

665 **Torres-Ruiz JM, Cochard H, Mayr S, Beikircher B, Diaz-Espejo A, Rodriguez-**
666 **Dominguez CM, Badel E, Fernández JE. 2014.** Vulnerability to cavitation in
667 *Olea europaea* current-year shoots: further evidence of an open vessel artefact
668 associated with centrifuge and air-injection techniques. *Physiologia Plantarum*
669 **152**: 465–474.

670 **Torres-Ruiz JM, Cochard H, Mencuccini M, Delzon S, Badel E. 2016**. Direct
671 observation and modelling of embolism spread between xylem conduits: a case
672 study in Scots pine. *Plant, Cell & Environment* **39,** 2774–2785.

673 **Torres-Ruiz JM, Diaz-Espejo A, Morales-Sillero A, Martín-Palomo MJ, Mayr S,**
674 **Beikircher B, Fernández JE. 2013.** Shoot hydraulic characteristics, plant water
675 status and stomatal response in olive trees under different soil water conditions.
676 *Plant and Soil* **373**: 77–87.

677 **Torres-Ruiz JM, Diaz-Espejo A, Perez-Martin A, Hernandez-Santana V. 2015b.**
678 Role of hydraulic and chemical signals in leaves, stems and roots in the stomatal
679 behaviour of olive trees under water stress and recovery conditions. *Tree*
680 *Physiology* **35**: 415–424.

681 **Torres-Ruiz JM, Jansen S, Choat B, McElrone AJ, Cochard H, Brodribb TJ,**
682 **Badel E, Burlett R, Bouche PS, Brodersen CR, Li S, Morris H, Delzon S.**
683 **2015a.** Direct X-Ray Microtomography Observation Confirms the Induction of
684 Embolism upon Xylem Cutting under Tension. *Plant Physiology* **167**: 40–43.

685 **Torres-Ruiz JM, Sperry JS, Fernández JE. 2012.** Improving xylem hydraulic
686 conductivity measurements by correcting the error caused by passive water
687 uptake. *Physiologia Plantarum* **146**: 129–135

688 **Trifilò P, Raimondo F, Lo Gullo MA, Barbera PM, Salleo S, Nardini A. 2014.**
689 Relax and refill: xylem rehydration prior to hydraulic measurements favours
690 embolism repair in stems and generates artificially low PLC values. *Plant, Cell*
691 *& Environment* **37**: 2491–2499.

Tyree MT, Zimmermann MH. 2002. Xylem structure and ascent of sap. Springer, Berlin, Germany.

Urli M, Porté AJ, Cochard H, Guengant Y, Burlett R, Delzon S. 2013. Xylem embolism threshold for catastrophic hydraulic failure in angiosperm trees. *Tree Physiology* **33**: 1–12

Wheeler JK, Huggett BA, Tofte AN, Rockwell FE, Holbrook NM. 2013. Cutting xylem under tension or supersaturated with gas can generate PLC and the appearance of rapid recovery from embolism. *Plant, Cell & Environment* **36**: 1938–1949.

Zimmermann MH, Jeje AA. 1981. Vessel-length distribution in stems of some American woody plants. *Canadian Journal of Botany* **59**, 1882–1892.

Tables

Table 1: Overview of the species studied with reference to their sample length, mean native xylem water potentials before taking specific hydraulic conductivity measurements, and the pressure induced by centrifugation using the Cavitron or the original rotor design (i.e. Alder *et al*., 1997 design). Values indicate mean ± standard error.

	Sample length (cm)		**Native xylem water potentials** (MPa, mean ± SE ; *n*)		**Induced pressure** (MPa)
Species	Cavitron	Original	Cavitron	Original	
Betula pendula	40	15	-2.1 ± 0.1 ; 6	-1.8 ± 0.0 ; 6	-1.5
Olea europaea	15	15	-2.4 ± 0.1 ; 7	-2.0 ± 0.1 ; 6	-1.5
Quercus palustris	15	15	-2.5 ± 0.2 ; 6	-2.0 ± 0.1 ; 6	-1.5

Figure Legends

Fig. 1. Two contrasting curves showing the predicted loss in K_s according to the 's-shaped' and 'r-shaped' scenario. Resistance to xylem embolism has typically been evaluated by inducing lower xylem pressures progressively and determining their corresponding losses in K_s (closed circles), which makes it difficult to distinguish between real and artefactual loss in K_s (closed circle 'a' to 'b'). By exposing a sample to a less negative pressure, i.e. nearer to zero, than the minimum pressure previously experienced, a decrease in K_s can be considered as artefactual (open circle 'a' to 'b') since less negative pressures cannot induce embolism (open circle 'a' to 'c').

Fig. 2 Percentage of open vessels (i.e., open at both sample ends) in 15cm-long samples of *Olea europaea* and *Quercus palustris*. There are no data for *Betula pendula* since no open vessels were detected in either the 15 cm-long samples or the 40 cm-long ones for this species. Each column is the average of four samples per species and vertical bars represent ± the standard error.

Fig. 3. Mean specific hydraulic conductivity (K_s) for *Betula pendula*, *Olea europaea* and *Quercus palustris* xylem samples before (NP, 'native xylem pressure) and after spinning in a rotor according to the Cavitron (panels on the left) or the original rotor design (Alder et al. 1997; panels on the right) to induce a less negative xylem pressure (-1.5 MPa, AS, 'after spinning') than the minimum pressure previously experienced by the plant. Each column is the average of *n* samples per species and vertical bars represent the standard error. Significant differences between NP and AS are indicated as $p<0.05$ or $p<0.01$; *n.s.* indicates no significant differences.

Fig. 4 a) Mean specific hydraulic conductivity (K_s) for *Betula pendula*, *Olea europaea* and *Quercus palustris* girdled and control (i.e. non-girdled) xylem samples after xylem pressure relaxation. **b)** Specific hydraulic conductivity (K_s) for *Olea europaea* measured before (K_{s1}) and after (K_{s2}) disconnecting the samples, leaving them to sit in water for an equivalent time as those that were spun (i.e. 5 min) and reconnecting them to the tubing conductivity apparatus. Each column is the average of *n* samples per species and vertical bars represent the standard error. *n.s.* indicates no significant differences (i.e. $p>0.05$).

Fig. 5 Transverse micro-CT images of *Olea europaea* at different xylem water potentials (Ψ_{xyl}, bottom of each picture). Embolised vessels are observed as black. The percentage loss of hydraulic conductivity (PLC) is indicated for each sample. Scale bar = 500 μm.

Fig. 6 Vulnerability curve obtained by direct observation (micro-CT) from intact olive plants (full, black dots correspond to individual PLC measurements based on scans, and the solid black line to the Weibull fitting). The grey dashed line represents the tangent through the midpoint of the vulnerability curve and its x-intercept represents the air entry pressure (P_e) according to Meinzer *et al.* (2009).

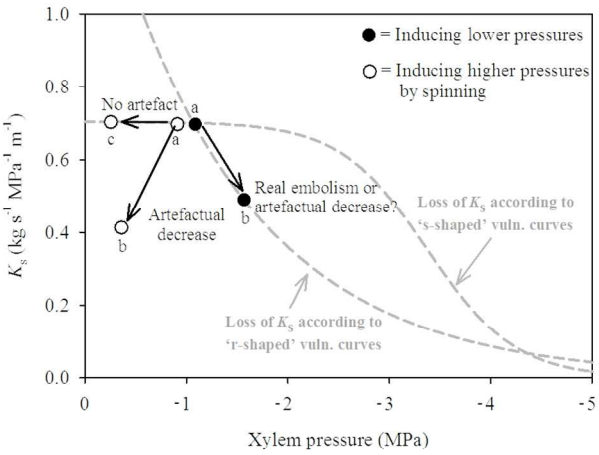

Fig. 1. Two contrasting curves showing the predicted loss in K_s according to the 's-shaped' and 'r-shaped' scenario. Resistance to xylem embolism has typically been evaluated by inducing lower xylem pressures progressively and determining their corresponding losses in K_s (closed circles), which makes it difficult to distinguish between real and artefactual loss in K_s (closed circle 'a' to 'b'). By exposing a sample to a less negative pressure, i.e. nearer to zero, than the minimum pressure previously experienced, a decrease in K_s can be considered as artefactual (open circle 'a' to 'b') since less negative pressures cannot induce embolism (open circle 'a' to 'c').

210x296mm (150 x 150 DPI)

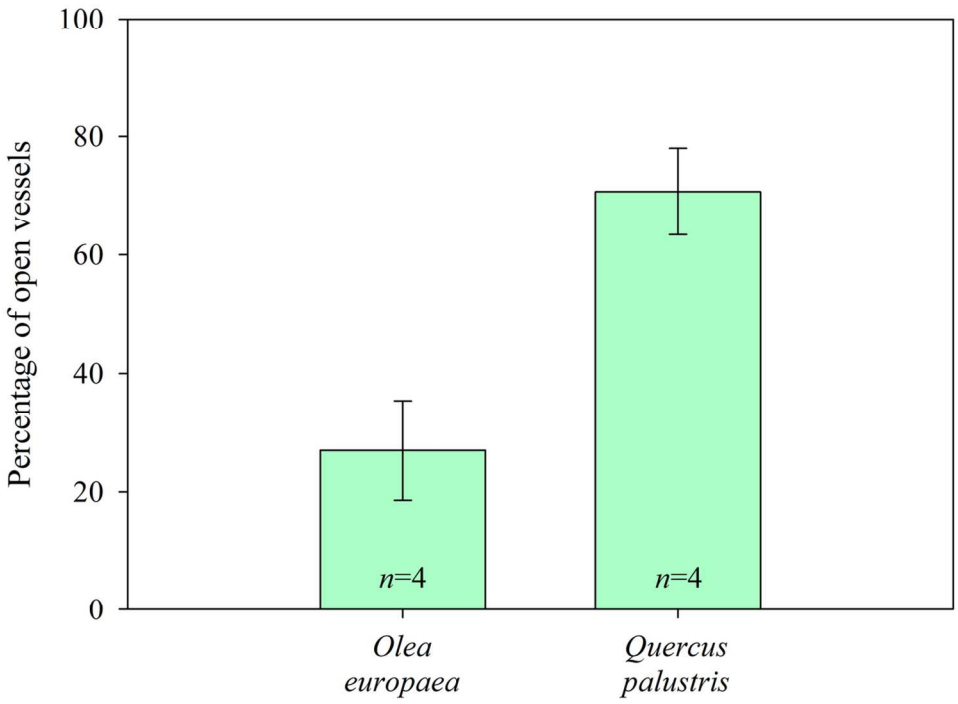

Fig. 2. Percentage of open vessels (i.e., open at both sample ends) in 15cm-long samples of *Olea europaea* and *Quercus palustris*. There are no data for *Betula pendula* since no open vessels were detected in either the 15 cm-long samples or the 40 cm-long ones for this species. Each column is the average of four samples per species and vertical bars represent ± the standard error.

116x89mm (300 x 300 DPI)

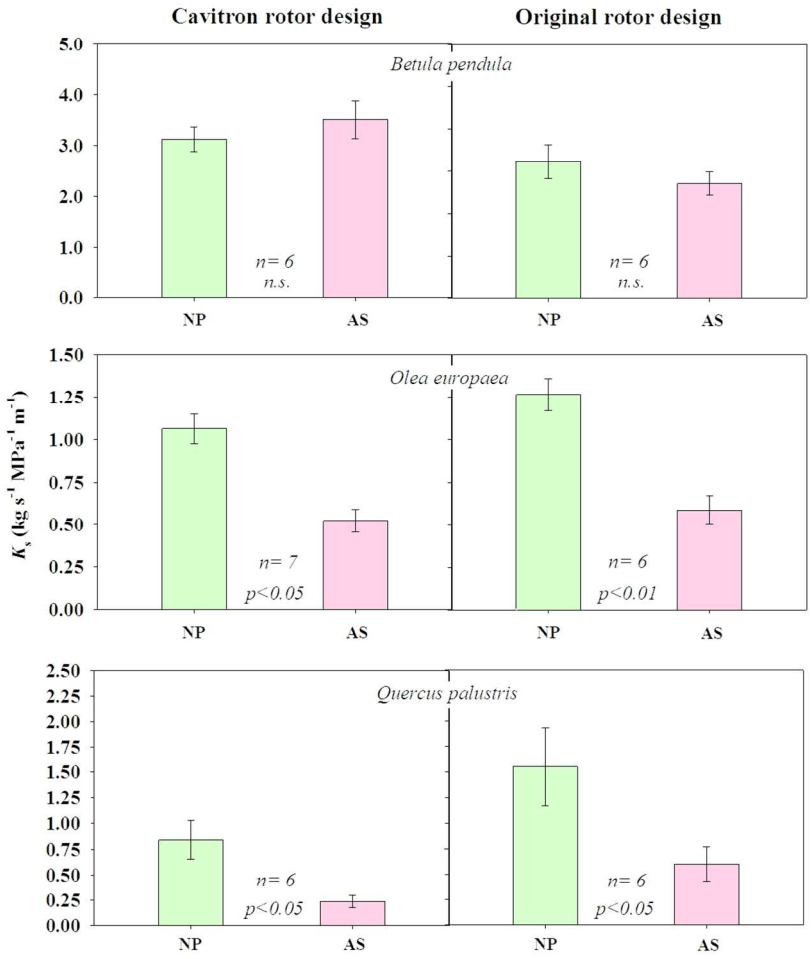

Fig. 3. Mean specific hydraulic conductivity (K_s) for *Betula pendula*, *Olea europaea* and Quercus palustris xylem samples before (NP, 'native xylem pressure) and after spinning in a rotor according to the Cavitron (panels on the left) or the original rotor design (Alder *et al.* 1997; panels on the right) to induce a less negative xylem pressure (-1.5 MPa, AS, 'after spinning') than the minimum pressure previously experienced by the plant. Each column is the average of *n* samples per species and vertical bars represent the standard error. Significant differences between NP and AS are indicated as $p<0.05$ or $p<0.01$; *n.s.* indicates no significant differences.

210x296mm (150 x 150 DPI)

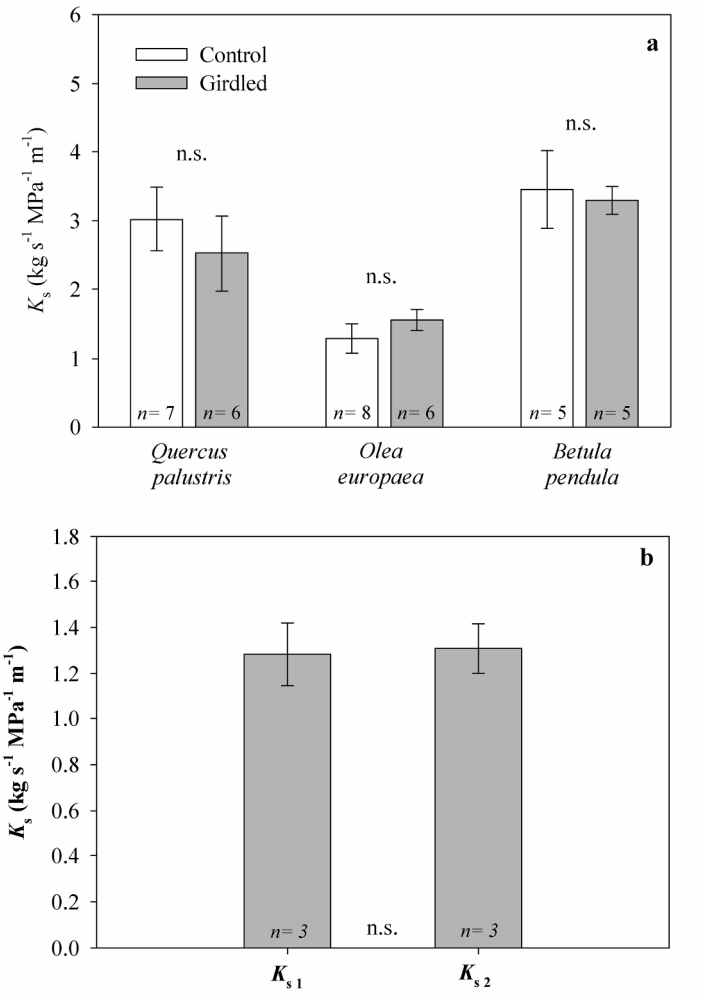

Fig. 4. a) Mean specific hydraulic conductivity (K_s) for *Betula pendula*, *Olea europaea* and *Quercus palustris* girdled and control (i.e. non-girdled) xylem samples after xylem pressure relaxation. b) Specific hydraulic conductivity (K_s) for *Olea europaea* measured before (K_{s1}) and after (K_{s2}) disconnecting the samples, leaving them to sit in water for an equivalent time as those that were spun (i.e. 5 min) and reconnecting them to the tubing conductivity apparatus. Each column is the average of *n* samples per species and vertical bars represent the standard error. *n.s.* indicates no significant differences (i.e. $p>0.05$).

175x298mm (300 x 300 DPI)

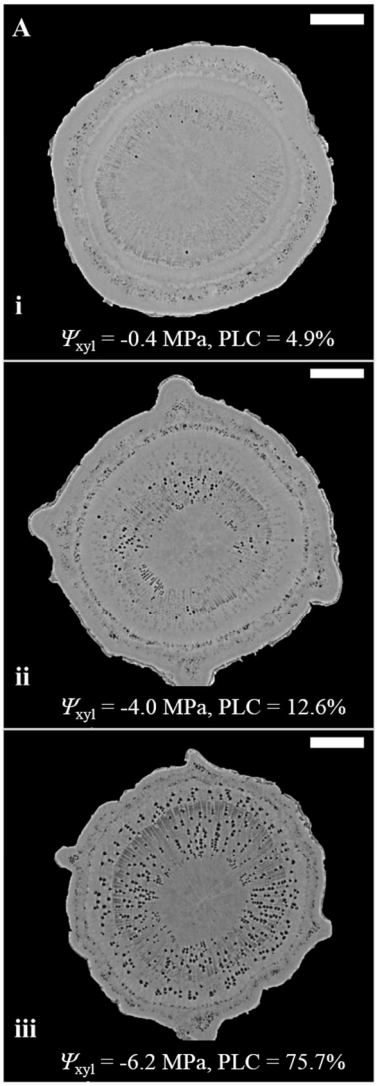

Fig. 5. Transverse micro-CT images of *Olea europaea* at different xylem water potentials (Ψ_{xyl}, bottom of each picture). Embolised vessels are observed as black. The percentage loss of hydraulic conductivity (PLC) is indicated for each sample. Scale bar = 500 μm.

91x254mm (150 x 150 DPI)

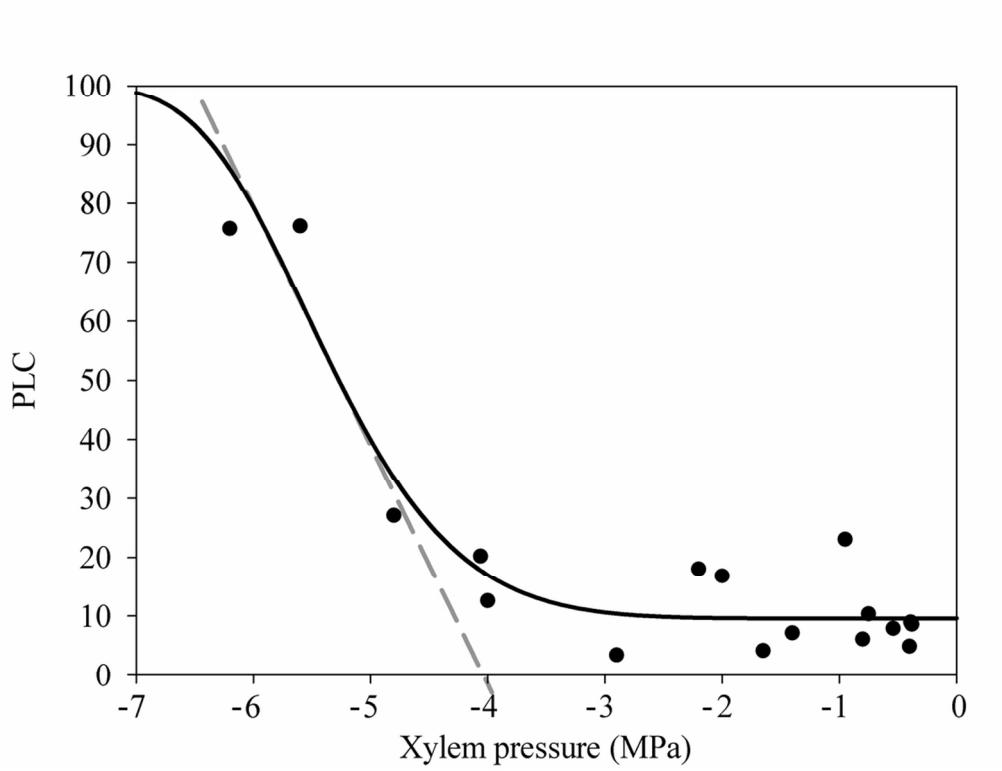

Fig. 6. Vulnerability curve obtained by direct observation (micro-CT) from intact olive plants (full, black dots correspond to individual PLC measurements based on scans, and the solid black line to the Weibull fitting). The grey dashed line represents the tangent through the midpoint of the vulnerability curve and its x-intercept represents the air entry pressure (P_e) according to Meinzer *et al.* (2009).

100x77mm (300 x 300 DPI)